

# The Effect of GPS Parameters on Mechanical Properties of Y- $\alpha$ -SiAlON Ceramics

H. X. Li,<sup>a</sup> W. Y. Sun,<sup>a</sup> P. L. Wang,<sup>a</sup> D. S. Yan<sup>a</sup> & T. Y. Tien<sup>b</sup>

<sup>a</sup>Shanghai Institute of Ceramics, Chinese Academy of Sciences, Shanghai 200050, P.R. China

<sup>b</sup>Materials Science and Engineering Department, University of Michigan, Ann Arbor, MI 48109, USA

(Received 5 October 1995; accepted 3 January 1996)

**Abstract:** A dense, oxygen-rich Y- $\alpha$ -sialon ceramic, with a small amount of YAG as a grain boundary phase, has been fabricated through GPS (gas pressure sintering). The effect of nitrogen pressure during GPS on densities and mechanical properties of the materials has been studied, which was observed to be relevant to the YAG content. The  $\alpha$ -sialon with 2.5 wt% YAG, GPSed under 3 MPa and at 1800°C, possesses a flexural strength of 500 MPa, hardness (Vickers) of 1816 kg mm<sup>-2</sup> and fracture toughness (K<sub>1c</sub>) of 3.4 MPa·m<sup>1/2</sup>. © 1997 Elsevier Science Limited and Techna S.r.l.

## 1 INTRODUCTION

$\alpha$ -Sialon (or  $\alpha'$ ), a solid solution based on the structure of  $\alpha$ -Si<sub>3</sub>N<sub>4</sub> with a chemical composition of  $M_x\text{Si}_{12-(m+n)}\text{Al}_{m+n}\text{O}_n\text{N}_{16-n}$  ( $M = \text{Y, Ln, Ca, Mg, Li...}$ ), has been well known to be a promising engineering material, capable of being used as cutting tips because of the high hardness and better thermal shock resistance of  $\alpha'$  phase. The very low diffusivity in covalently bonded Si<sub>3</sub>N<sub>4</sub>, which leads to the difficulty in full densification of Si<sub>3</sub>N<sub>4</sub>-based ceramics, has annoyed the researchers working on silicon nitride ceramics with high performance. One conventional approach is to put oxide additives to promote densification by forming liquid phase with the SiO<sub>2</sub> (on the surface of Si<sub>3</sub>N<sub>4</sub> powder). The liquid phase, however, remains as a glassy phase at the grain boundaries after cooling down and deteriorates the high temperature mechanical properties of the materials. In recent years, GPS has proved to be an effective approach to minimize the content of oxide additives at no sacrifice of density, because high nitrogen pressure is of advantage for suppressing decomposition of Si<sub>3</sub>N<sub>4</sub> at temperatures above 1800°C, and for providing extra driving force for sintering.<sup>1–3</sup>

Phase relationships in the Y-Si-Al-O-N system<sup>4</sup> indicate that whole  $\alpha$ -sialon compositions are compatible with melilite, but there exists a tie-line between oxygen-rich  $\alpha$ -sialon ( $m=1, n=1.7$ ) and YAG, forming  $\alpha'$  ( $m=1, n=1.7$ )- $\beta_{10}(z=0.8)$ -12H (AlN-polytypoid phase)-YAG compatibility tetrahedron (see Fig. 1). These phase relationships provide the possibility to fabricate  $\alpha'$  or  $\alpha'$ - $\beta'$  or  $\alpha'$ -12H ceramics with YAG as a grain boundary phase. In our previous work, an  $\alpha'$ - $\beta'$ -YAG composite sialon material with high mechanical performance was fabricated through GPS.<sup>5</sup> Current work has focused on the fabrication and mechanical properties of  $\alpha$ -sialon ceramics through GPS.

## 2 EXPERIMENTAL

The starting materials used were Si<sub>3</sub>N<sub>4</sub> (LC12, Starck), AlN (1–2  $\mu\text{m}$ , 1.2 wt% oxygen, Zhuzhou Institute of Hard Metals, China), Al<sub>2</sub>O<sub>3</sub> (99.99%) and Y<sub>2</sub>O<sub>3</sub> (99.9%). The oxygen content on the surface of nitrides was taken into account when making the composition. The mixed powder with an  $\alpha$ -sialon composition of Y<sub>0.33</sub>Si<sub>9.3</sub>Al<sub>2.7</sub>O<sub>1.7</sub>N<sub>14.3</sub> and YAG (1 and 2.5 wt%, corresponding to no. 1

and no. 2, respectively, in Table 1) was ball-milled with absolute alcohol for 24 h, dried and passed through 120-mesh screen, and then die-pressed followed by cold isostatic pressing into testing bars. The reaction sequence and densification were performed in a graphite-resistance furnace under 1 atm. of  $N_2$  while holding for 5 min at intervals of

100°C in the range 1450–1800°C. A GPS furnace with graphite-resistance was used to sinter the specimens under nitrogen pressures of 1, 3 and 5 MPa, respectively. A two-step firing schedule (0.4 MPa, 1650°C–2 h and given pressure, 1800°C–2 h) was used. For comparison, the same compositions were also sintered under flowing  $N_2$  (1 atm.)

Table 1. The starting compositions and phases present after PLS at 1800°C for 2 h

| Specimen no. | Starting compositions          |      |                                |                               | Phase compositions                    |  |
|--------------|--------------------------------|------|--------------------------------|-------------------------------|---------------------------------------|--|
|              | Si <sub>3</sub> N <sub>4</sub> | AlN  | Al <sub>2</sub> O <sub>3</sub> | Y <sub>2</sub> O <sub>3</sub> | Before H.T.                           | After H.T.                             |
| 1            | 73.3                           | 16.1 | 3.7                            | 6.9                           | $\alpha'$ s; AlN tr.                  | $\alpha'$ s; YAG vw; AlN tr.           |
| 2            | 72.2                           | 15.8 | 4.3                            | 7.7                           | $\alpha'$ s; $\beta'$ w; 12H vw; B vw | $\alpha'$ s; $\beta'$ w; YAG w; 12H vw |

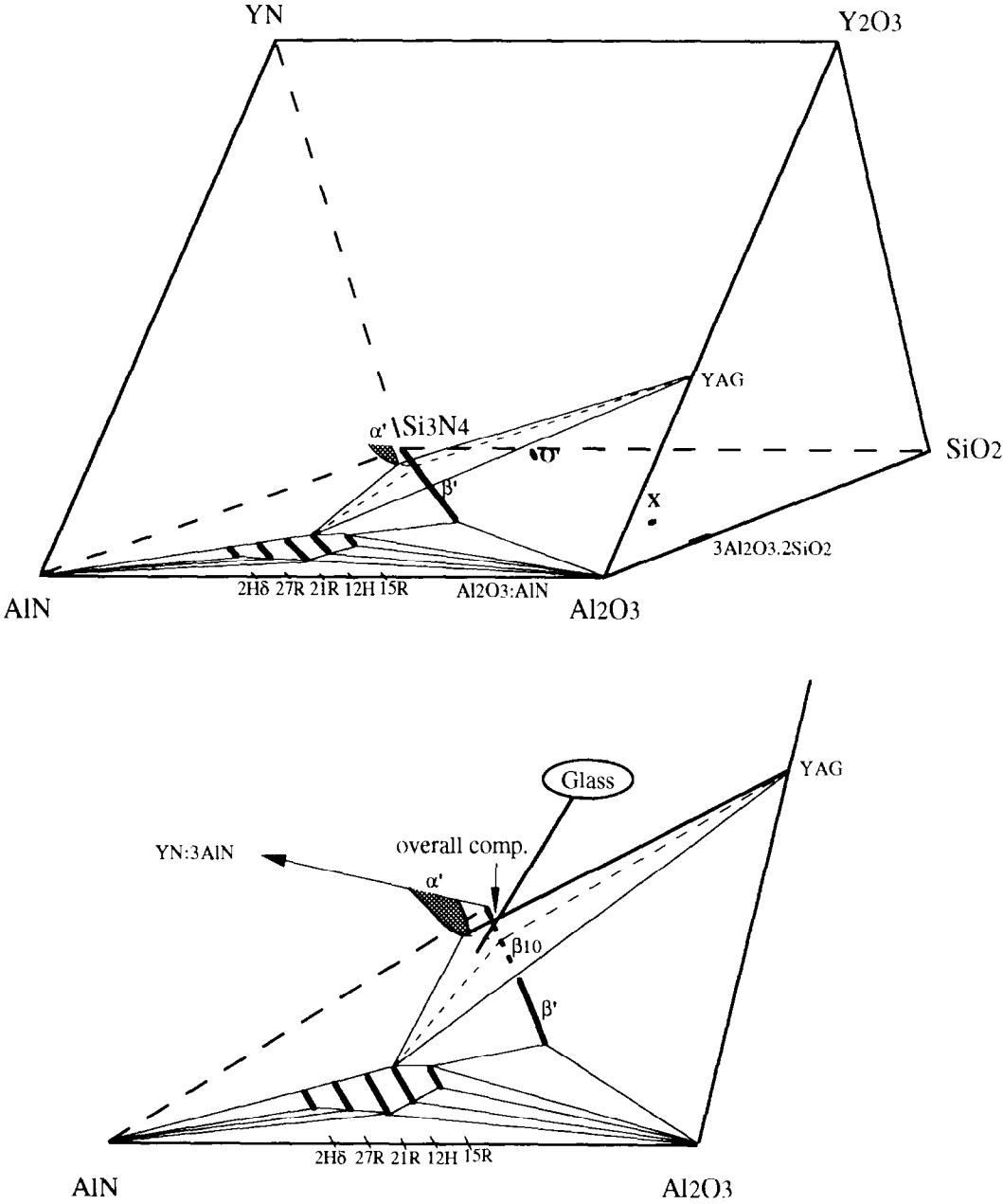


Fig. 1. Representation of Y-sialon system showing phase diagram of Si–Al–O–N and the  $\alpha'$  ( $m=1, n=1.7$ )– $\beta_{10}$ –12H–YAG compatibility tetrahedron (top diagram); the enlarged region around overall composition showing the tie-line of  $\alpha'$ –YAG rotating towards glass (bottom diagram).

at 1800°C. The phases were identified by X-ray diffraction technique. Hardness and indentation fracture toughness were measured by using a diamond indenter under a load of 100 N. Flexural strength was tested by three-point bending with a 30 mm span (20 mm for high temperature test) and a cross-head speed of 0.5 mm/min. Both polished and fractured surfaces were observed by SEM. A TEM study was also performed to reveal the grain

boundary structure for the specimens after heat treatment at 1250°C for 24 h.

### 3 RESULTS AND DISCUSSION

Prior to studying the fabrication of an  $\alpha$ -sialon ceramic material under high pressure nitrogen, some behaviours, such as the formation of  $\alpha$ -sialon

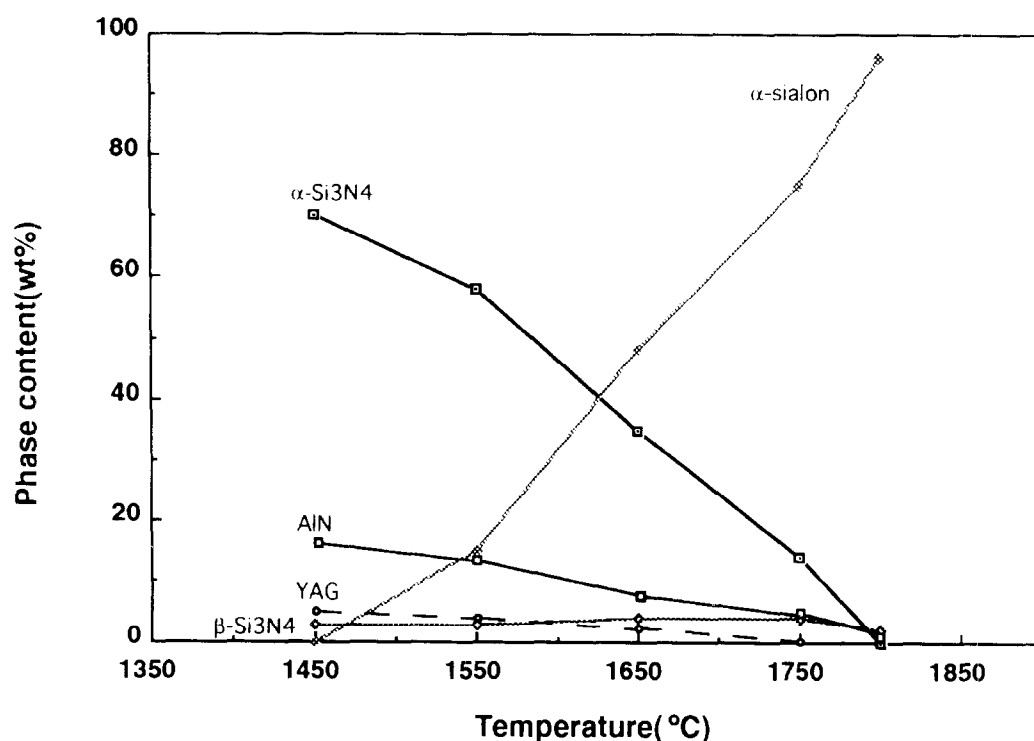


Fig. 2. Reaction sequence of  $Y$   $\alpha$ -sialon composition with 1 wt% YAG (no. 1).

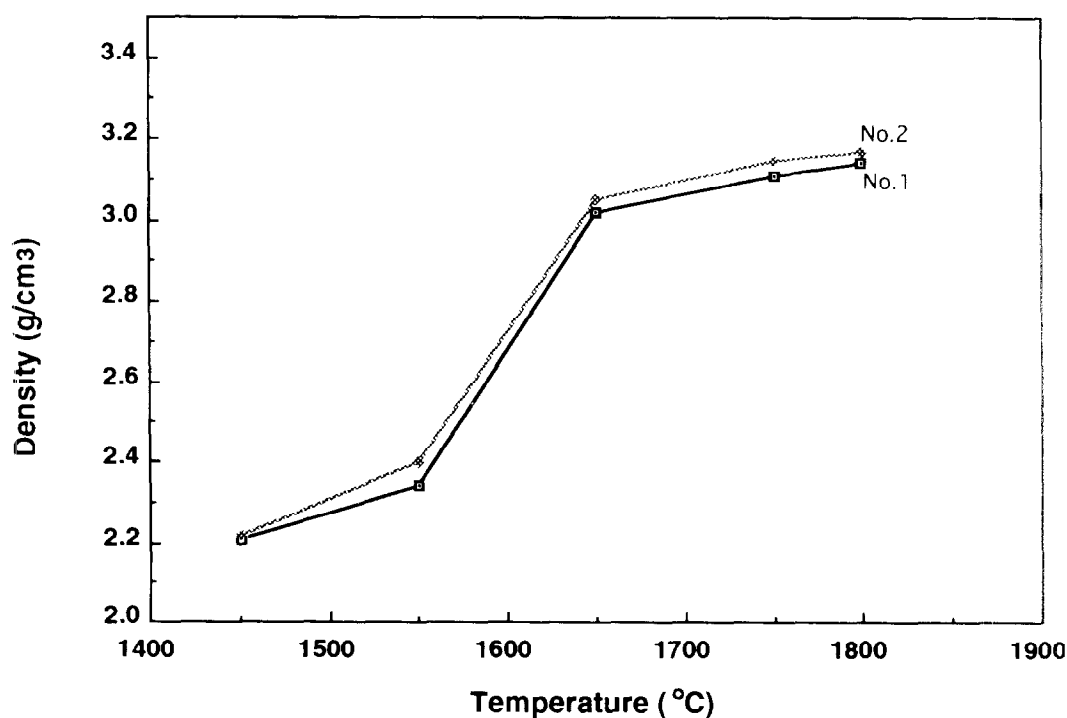


Fig. 3. Densification behaviour of compositions no. 1 (1 wt% YAG) and no. 2 (2.5 wt% YAG).

occurring under 1 atm. ( $N_2$ ), are still required to be understood for reference. The formation of Y- $\alpha$ -sialons studied in our previous work,<sup>6,7</sup> indicates that the ratio of  $\alpha'/\beta'$  and transient Y-containing phases are apparently relevant with the compositions. Therefore, the reaction sequences of the compositions under study were determined again. The results show that in the formation of  $\alpha$ -sialon, these two compositions (1% and 2.5% YAG) are very similar, except for a small amount of  $\beta$ -sialon left in the composition with 2.5% YAG (no. 2). The reaction sequences (no. 1) and densification behaviours are represented in Figs 2 and 3. Obviously, the big change in densification occurs at 1550–1700°C, where  $\alpha$ -sialon is formed dramatically. The final phase compositions after firing at 1800°C for 2 h are listed in Table 1. As indicated, YAG crystallizes out after heat treatments (1250°C–24 h) and monophase  $\alpha'$  only occurs in composition no. 1 (1% YAG). The occurrence of  $\beta$ -sialon in the  $\alpha'$  compositions has always been observed, especially in Ln- $\alpha'$  compositions with a lower Z-value of Ln elements.<sup>7</sup> The formation of either Ln-melilite or liquid phase, which exhaust the Ln or Y level designed for making up  $\alpha'$ , results in the production of  $\beta$ -sialon. For the compositions under study, the formation of Y-sialon glass is the case. The overall compositions were designed on the tie-line between  $\alpha'$  and YAG, but the formation of glassy phase made the  $\alpha'$ -YAG tie-line rotate

towards glass and the other terminal point shift towards the  $\alpha'-\beta'$  or  $\alpha'-\beta'-12H$  phase regions (see Fig. 1). The compositions in these regions contain less Y than  $\alpha'$ , thus compensating for the extra yttrium dissolved in the glassy phase. B-phase (Table 1) is an yttrium aluminium silicon oxynitride (with the composition of  $Y_2SiAlO_5N$ ), which normally crystallizes out from Y-sialon glasses during slow cooling or heat treatment at lower temperatures (1050°C).<sup>8</sup> The occurrence of this phase in composition no. 2 also indicates that more glassy phase is involved in this composition.

It has been well established that the high pressure of nitrogen has the effect of suppressing decomposition of silicon nitride and also giving extra sintering driving force. As expected, in the present experiment, the weight losses occurring under high pressures are all less than 1%, while the pressure-less sintering gives a weight loss of around 2.5–3.0%. The driving force of gas pressure for densification is also apparent. As indicated in Table 2, the densities, achieved under 1 MPa and at 1700°C, are all higher than those obtained at 1800°C (0.1 MPa) (Table 3). Composition no. 1, sintered at 1800°C, has very low density (96.2%), but it can reach a value of 98.2% dense when 1 MPa (1800°C) is applied. The densities and mechanical performance achieved under gas pressures are summarised in Tables 3 and 4 and Figs 4 and 5. As observed in other researchers' work,<sup>9</sup> in some

Table 2. The effect of temperature on densities and mechanical properties

| Sintering condition             | 1700°C–2 h, 1 MPa |         | 1800°C–2 h, 1 MPa |         | 1800°C–2 h, PLS |         |
|---------------------------------|-------------------|---------|-------------------|---------|-----------------|---------|
| Sample no.                      | 1                 | 2       | 1                 | 2       | 1               | 2       |
| $D/D_{th}$ (%)                  | 97.5              | 98.8    | 98.2              | 99.3    | 96.2            | 98.2    |
| $H_{v10}$ (kg/mm <sup>2</sup> ) | 1572±31           | 1624±46 | 1687±5            | 1935±50 | 1341±10         | 1546±20 |
| $K1c$ (MPa·m <sup>1/2</sup> )   | 4.2±0.1           | 3.8±0.2 | 4.1±0.2           | 3.8±0.2 | —               | 3.6±0.2 |

Table 3. The effect of nitrogen pressure (at 1800°C) on densities and phase compositions

| Pressure (MPa) | $D/D_{th}$ (%) |       | Phase compositions    |  |
|----------------|----------------|-------|-----------------------|--|
|                | No. 1          | No. 2 | No. 1                 | No. 2                                  |
| 0.1            | 96.2           | 98.2  | $\alpha'$ vs; AlN tr. | $\alpha'$ vs; $\beta'$ w; 12H vw; B vw |
| 1.0            | 98.0           | 99.3  | $\alpha'$ vs; 12H tr. | $\alpha'$ vs; 12H w; $\beta'$ vw       |
| 3.0            | 99.2           | 99.2  | $\alpha'$ vs; 12H tr. | $\alpha'$ vs; 12H w; $\beta'$ vw       |
| 5.0            | 99.5           | 98.5  | $\alpha'$ vs; 12H tr. | $\alpha'$ vs; 12H w; $\beta'$ vw       |

Table 4. The effect of nitrogen pressure (at 1800°C) on mechanical properties

| Pressure (MPa) | $K1c$ (MPa·m <sup>1/2</sup> ) |         | $\sigma_t$ (MPa) |        | $H_{v10}$ (kg/mm <sup>2</sup> ) |         |
|----------------|-------------------------------|---------|------------------|--------|---------------------------------|---------|
|                | No. 1                         | No. 2   | No. 1            | No. 2  | No. 1                           | No. 2   |
| 0.1            | 5.3±0.2                       | 3.6±0.2 | —                | 421±34 | 1341±10                         | 1546±20 |
| 1.0            | 4.1±0.2                       | 3.8±0.2 | 414±24           | 437±17 | 1687±5                          | 1935±50 |
| 3.0            | 3.5±0.1                       | 3.4±0.2 | 454±21           | 500±12 | 1732±20                         | 1816±11 |
| 5.0            | 3.8±0.1                       | 3.4±0.2 | 467±30           | 474±3  | 1875±42                         | 1728±13 |

cases, when the nitrogen pressure is raised up to a certain level, it would have an adverse effect on densification and mechanical properties. This is because some pores originally existing in the green body or caused by vaporization of liquid phase at high temperatures can not be eliminated under high pressure. Therefore, the effect of nitrogen pressure on densification and properties is strongly

dependent on experimental conditions and the compositions of the materials. As indicated, composition no. 1 (1% YAG) has increasing density with increasing nitrogen pressure, but the peak density (99.3%) in composition no. 2 occurs at pressures of around 1-3 MPa. It has been well known that the mechanical performances of ceramic materials are closely dependent on their

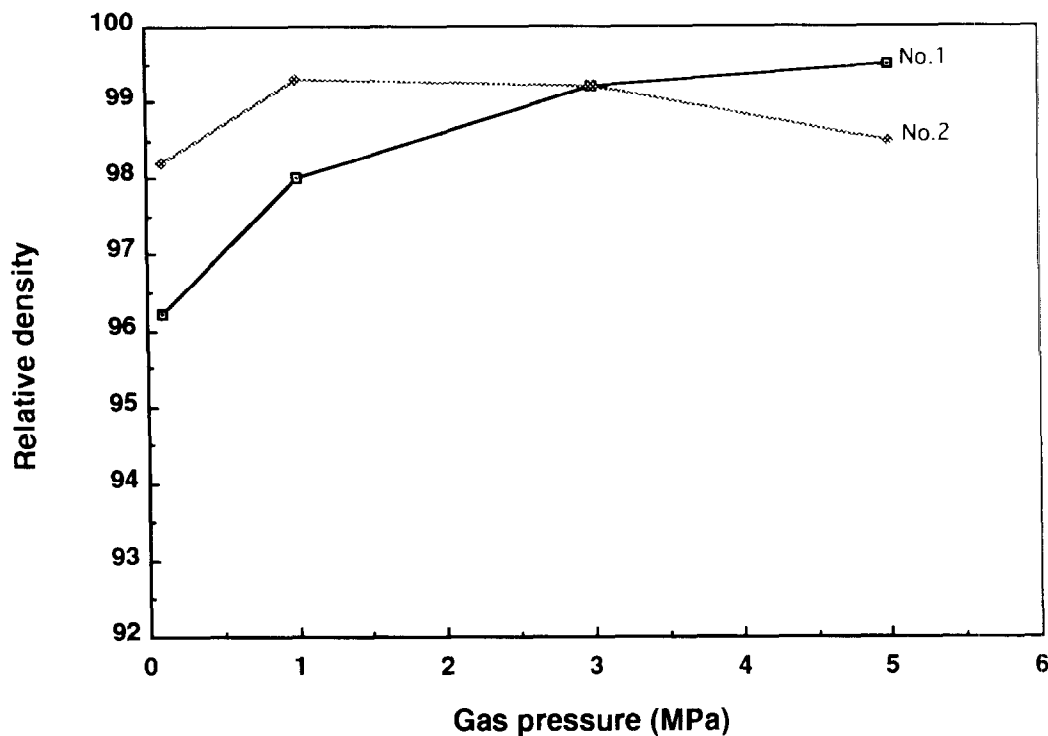


Fig. 4. Effect of gas pressure on densities.

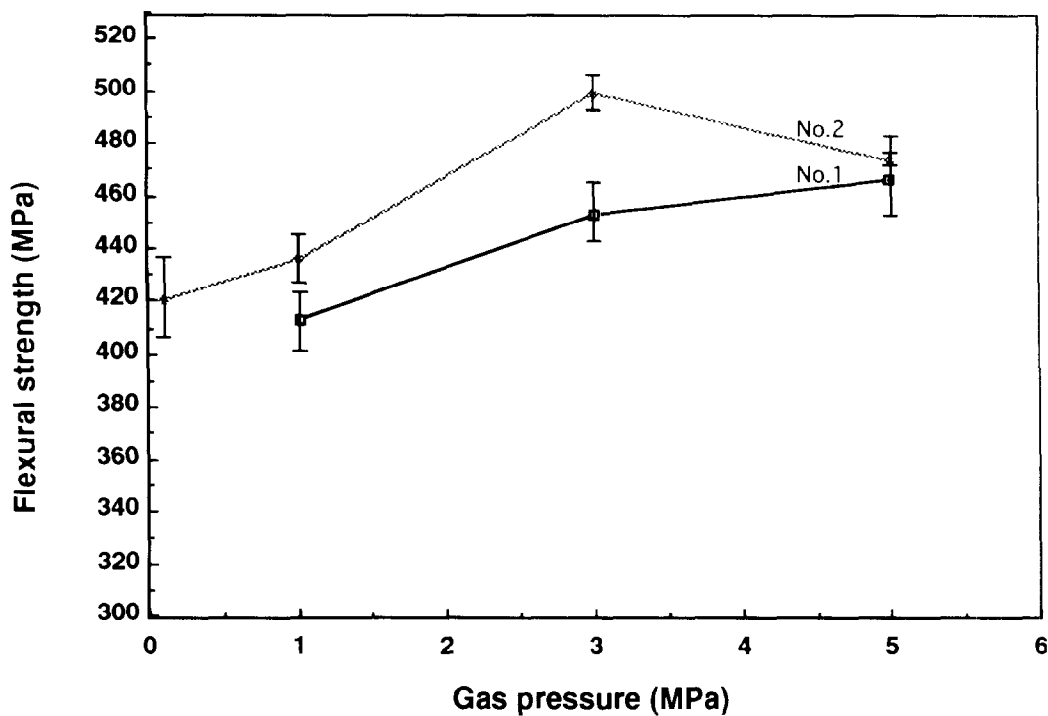


Fig. 5. Effect of gas pressure on flexural strength.

densities and microstructures. As indicated, the variation tendency of hardness is in good agreement with densities. However, the strength and fracture toughness are more sensitive to their microstructures. Figures 6 and 7 compare the microstructures formed through GPS and PLS, respectively. The microstructures developed under 3 MPa (Fig. 6) are more homogeneous and contain less pores than those that were pressureless sintered (Fig. 7). Composition no. 1 contains less liquid phase and is composed of slightly larger grains and this probably results in its slightly lower strength, although it has the same density (99.2%) as composition no. 2 GPSed under the same conditions (3 MPa and 1800°C). Among these materials, the

specimens of composition no. 2 GPSed under 1–3 MPa have the optimum mechanical properties — a flexural strength of 500 MPa, fracture toughness of  $3.8 \text{ MPa}\cdot\text{m}^{1/2}$  and hardness of  $1935 \text{ kg/mm}^2$ . The SEM fracture surfaces of the materials GPSed (under 3 MPa), shown in Fig. 8, reveal the fracture occurring in intergranular model. This could be attributed to the small size and equiaxed grains of the  $\alpha$ -sialon materials. Figure 9 shows the TEM photographs of specimen no. 2, GASed under 3 MPa, and then heat treated at 1250°C for 24 h. These photos show the existence of YAG crystallized out at the isolated triple pockets and fibre-like 12H, as detected by the X-ray diffraction technique.

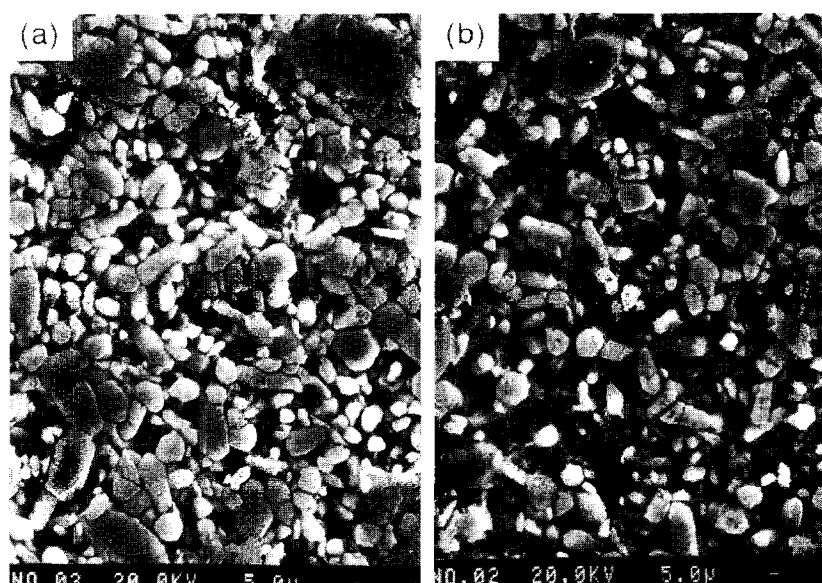


Fig. 6. SEM micrographs of GPSed specimens (1800°C, 3 MPa): (a) no. 1 (1 wt% YAG) and (b) no. 2 (2.5 wt% YAG).

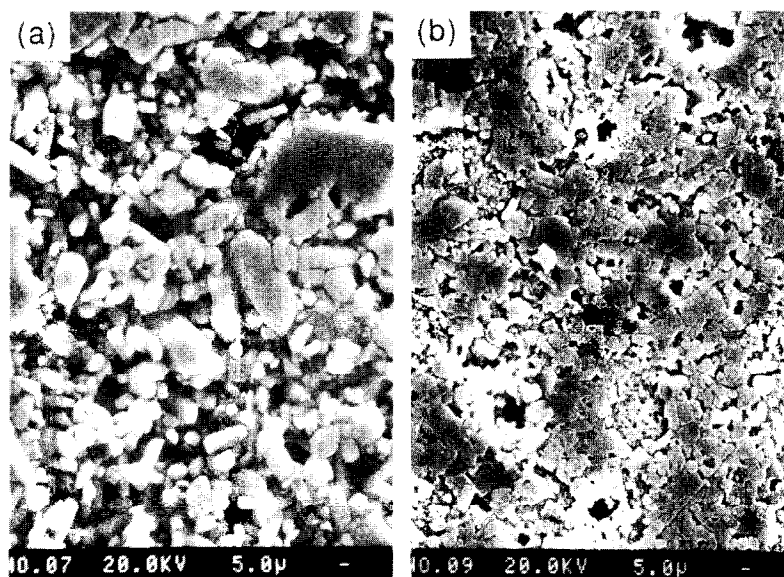


Fig. 7. SEM micrographs of specimens sintered at 1800°C: (a) no. 1 (1 wt% YAG) and (b) no. 2 (2.5 wt% YAG).

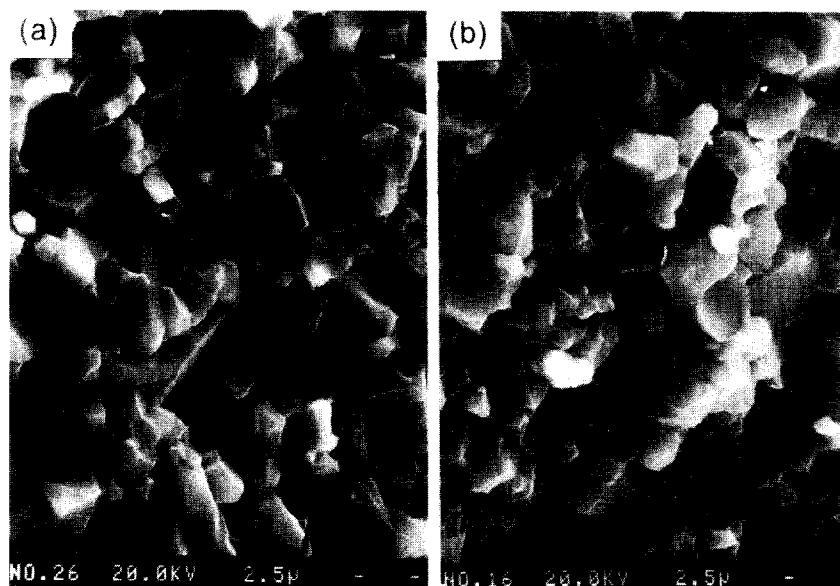


Fig. 8. SEM micrographs of fracture surfaces of GPSed specimens (1800 °C, 3 MPa): (a) no. 1 (1 wt% YAG) and (b) no. 2 (2.5 wt% YAG).

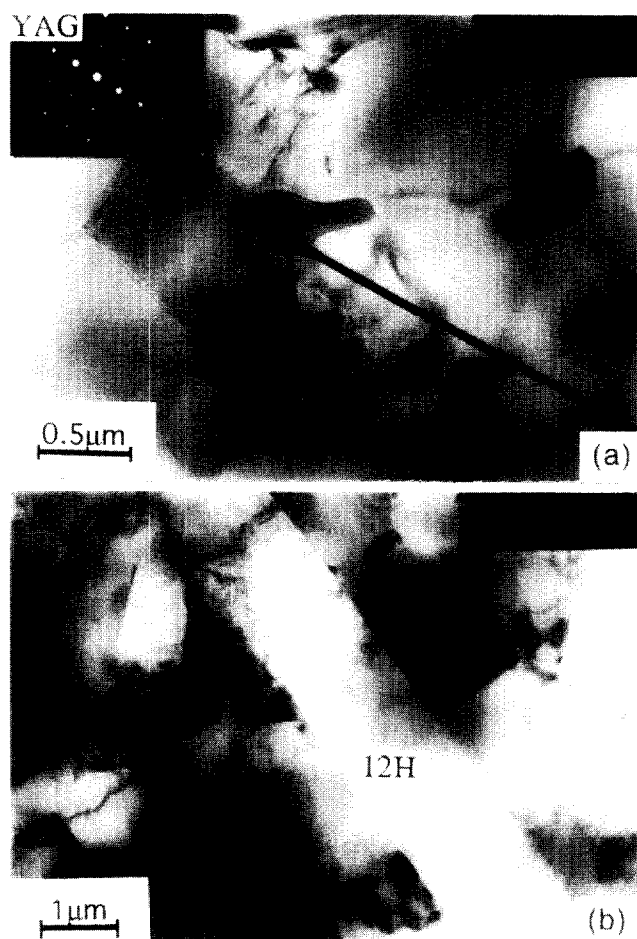


Fig. 9. TEM micrographs of composition no. 2, GPSed (under 3 MPa) and then heat treated, showing (a) YAG in the triple joints and (b) 12H.

#### 4 CONCLUSIONS

Dense, monophase, oxygen-rich  $\alpha$ -sialon ceramic materials, with a small amount of YAG (1–

2.5 wt%) as the grain boundary phase, have been fabricated through GPS. For the composition with 1.0% YAG, densities and mechanical properties increase with increasing nitrogen pressure. For the composition with more YAG (2.5%), the effect of nitrogen pressure on density and mechanical properties is not linear. The specimens of composition with 2.5% YAG, GPSed under 1–3 MPa (1800 °C), have the optimum mechanical properties—a flexural strength of 500 MPa, fracture toughness of  $3.8 \text{ MPa}\cdot\text{m}^{1/2}$  and hardness of  $1935 \text{ kg}\cdot\text{mm}^{-2}$ .

#### REFERENCES

1. MITOMO, M., Pressure sintering of  $\text{Si}_3\text{N}_4$ . *J. Mater. Sci.*, **11** (1976) 1103–1107.
2. PRIEST, H. F., PRIEST, G. L. & GASSA, G. E., Sintering  $\text{Si}_3\text{N}_4$  under high nitrogen pressure. *J. Am. Ceram. Soc.*, **60** (1977) 81.
3. COBLE, R. L., Reactive sintering. In *Sintering—Theory and Practice*, ed. D. Kolar, S. Pejovnik & M. M. Bistic. Elsevier Scientific Publishing Co., Amsterdam, 1982, pp. 145–151.
4. SUN, W. Y., TIEN, T. Y. & YEN, T. S. (Yan, D. S.), Solubility limits of  $\alpha'$ -SiAlON solid solutions in the system Si–Al–Y–N–O. *J. Am. Ceram. Soc.*, **74** (1991) 2547–2550.
5. WANG, H., WANG, P. L., SUN, W. Y., ZHUANG, H. R. & YAN, D. S., High performance of  $\alpha'$ - $\beta'$  SiAlON ceramics. In *Proc. 5th Int. Symp. on Ceramic Materials and Components for Engines*, ed. D. S. Yan, X. R. Fu & S. X. Shi. World Scientific, Singapore, 1995, pp. 215–219.
6. SUN, W. Y., WU, F. Y. & YAN, D. S., Studies of the formation of  $\alpha'$  and  $\alpha'$ - $\beta'$  sialon. *Mater. Lett.*, **6** (1987) 11–15.
7. WANG, P. L., SUN, W. Y. & YEN, T. S., Sintering and formation behaviour of  $R$ - $\alpha'$  sialons ( $R$ —Nd, Sm, Gd, Dy, Er and Yb). *Eur. J. Solid State Inorg. Chem.*, **31** (1994) 93–104.

8. THOMPSON, D. P., Phase relationships in Y-Si-Al-O-N ceramics. In *Proc. Int. Symp. Tailoring Multiphase and Composite Ceramics*, ed. R. E. Tressler, G. L. Messing, C. G. Pantano & R. E. Neunham. MRS 20, Plenum Press, New York, 1986, pp. 78-91.
9. LI, W. L., ZHUANG, H. R. & FU, X. R., Silicon nitride swirl lower-chamber fabricated by gas pressure sintering. In *Proc. 5th Int. Symp. on Ceramic Materials and Components for Engines*, ed. D. S. Yan, X. R. Fu & S. X. Shi. World Scientific, Singapore, 1995, pp. 763-766.